International of Journal of Pharmaceutics

Regular article

Possibility and effectiveness of drug delivery to skin by needle-free injector

Naoko Inoue[3], Hiroaki Todo[1], Dai Iidaka[1], Yoshihiro Tokudome[1], Fumie Hashimoto[1], Tohru Kishino[3], Kenji Sugibayashi[※, 1, 2]

[1]Faculty of Pharmaceutical Sciences, [2]Life Science Research Center, Josai University, 1-1 Keyakidai, Sakado, Saitama 350-0295, Japan
[3]Department of Pharmacy Services, Saitama Medical Center, 1981 Kamoda, Kawagoe, Saitama, Japan

*Corresponding author: sugib@josai.ac.jp

Abstract

We evaluated a needle-free injector (NFI), which has been studied as an administration device to the subcutaneous tissue, as a device to deliver drugs into skin tissues. ShimaJet® used for self-injection of insulin was selected as a spring-powered NFI in this study. Weak (NFI-w) and strong (NFI-s) injectors were evaluated. Rhodamine 6G, as a model compound, was injected onto the skin surface of hairless rats and the skin distribution and amount released from the skin of the compound were followed. A modified nozzle (able to inject at an angle of 45 degrees) was prepared in addition to the conventional dedicated nozzle. The spring constants, nozzle shapes and penetration enhancer, 1-[2-(decylthio)ethyl] azacyclopentane-2-one (HPE-101), affected not only the skin distribution, but also the release profiles of rhodamine 6G. In addition, the release profiles of rhodamine 6G after injection using NFI-w or NFI-s obeyed diffusion-controlled or membrane-controlled kinetics, respectively. This difference was probably due to the skin site (depth) of rhodamine 6G delivered by the NFI. Furthermore, HPE-101 increased the retention time of rhodamine 6G in the epidermis. The present results suggested that an NFI can be a useful tool for enhanced drug delivery into skin.

Key words: needle-free injection, transdermal drug delivery, ShimaJet®, systemic drug

delivery, local drug delivery, high molecular weight compounds.

1. Introduction

The transdermal drug delivery system (TDDS) has several advantages for avoidance of the hepatic first-pass effect of drugs, long-acting sustained release of drugs, improved patient compliance and painless administration. Furthermore, these ingenious matrix-typed and membrane-controlled transdermal patches provide safe drug delivery. The Food and Drug Administration has approved many new transdermal patches containing rivastigmine and rotigotine (anti-Parkinson's drug), selegiline (antidepressant drug), buprenorphine (painkiller) and methylphenidate (attention-deficit hyperactivity disorder) since the beginning of this century. These patches show high therapeutic effects in addition to scopolamine, nitroglycerine, isosorbide dinitrate, estradiol, testosterone and fentanyl patches by overcoming the primary barrier in the stratum corneum against drug entry through to the systemic circulation of topically applied drugs. In addition, physicochemical methods, such as electroporation, microneedle and needle-free injection, are becoming popular to overcome the primary barrier in the stratum corneum for poorly permeable drugs. Many devices, Powder jector™, Macroflux™ and Ionsis ™, have already been reported as effective tools to increase the skin permeation of drugs. Among these techniques, needle-free injectors (NFI) have been investigated as an administration device not only

for high molecular weight compounds like insulin and human-growth hormone, but also for vaccine and gene delivery (Imoto and Konishi, 2005; Jackson et al., 2001; Agerso et al., 2002). Drug administration using an NFI has advantages of painless and fearless injection (Jovanovic-Peterson et al., 1993; Theintz and Sizonenko, 1991) and the minimum skin damage caused by injection compared with a conventional needle injector. Furthermore, the onset of therapeutic effects after administration using an NFI was much faster than with transdermal patches (Inoue et al., 1996), because needle-free injection directly delivered the drug into deep skin or muscle. In this study, the possibility of drug delivery using needle-free injection, especially to skin tissues, was investigated to achieve long-term maintenance of drug concentration in the systemic circulation and long action of the therapeutic effects. ShimaJet® was selected as a spring-powered NFI that was used in clinical practice in Japan as an injection device for insulin. The effect of the spring constant in ShimaJet® was evaluated on the drug distribution in skin after topical injection. Furthermore, the drug release profile from the injection site in skin was also investigated to clarify the usefulness of the NFI as a new drug delivery tool.

2. Theoretical

2.1. Analysis of drug release

The drug release profile from the skin after needle-free injection was analyzed by the following eq. (1) (Ritger and Peppas, 1987).

$$Q = kt^n \tag{1}$$

where Q is the cumulative amount of drug released from skin, k is the release rate constant, t is time after injection and n is the release exponent. When the release exponent, n, has a value of 0.5, the drug release shows Fickian release that follows W.I. Higuchi equation (Higuchi, 1962). When the release exponent has a value greater than 0.5 ($0.5 < n < 1$), the release behaves as non-Fickian diffusion. When release data are $n = 1$, the profile shows zero-order release.

3. Materials and methods

3.1. Materials and animals

Rhodamine 6G was purchased from Tokyo Chemical Industry Co., Ltd (Tokyo, Japan). 1-[2-(Decylthio)ethyl] azacyclopentane-2-one (HPE-101) was a gift from Hisamitsu Pharmaceutical Co., Inc. (Tokyo, Japan). All other reagents and solvents were of reagent or HPLC grade, and were used without further purification. Male hairless rats (WBN/ILA-Ht, 200–250 g) were supplied either by the Life Science

Research Center, Josai University (Sakado, Saitama, Japan) or Ishikawa Experimental Animal Laboratory (Fukaya, Saitama, Japan).

3.2. Needle-free injector

The spring-powered ShimaJet® (Shimadzu Co., Ltd., Kyoto, Japan) used in clinical practice in Japan was selected as a model NFI. Two springs with different spring constants (10.6 N/mm: improved spring in ShimaJet® (NFI-w) and 15 N/mm: used in commercially available ShimaJet® (NFI-s)) were used to investigate the injection force and drug distribution in the skin. A disposable dedicated nozzle (Fig. 1a) was easily attached to ShimaJet® and solution was filled from the top of the nozzle. In addition to the disposable dedicated nozzle, the effect of nozzle shape on drug distribution in the skin was investigated using a modified nozzle (Fig. 1b). The modified nozzle made from brass with an angle of 45 degrees was used to inject drug solution into skin (Fig. 1b). These nozzles have the same fluid flow path width and orifice diameter.

Fig. 1

3.3. Measurement of injection force

The injection force produced by ShimaJet® was measured by a TX-9A system (Fujimoto Laboratory, Tokyo, Japan). Figure 2 shows a diagram of the TX-9 system, which was composed of a measurement stand with i) a digital oscilloscope (DL716; Yokogawa Electric Co. Inc., Tokyo, Japan), ii) a sensor amplifier (DA-16A) and a sensor (TX-9UA). TX-9UA was divided into two main parts (Fig. 2b). The upper part (Fig. 2b) was a base to set ShimaJet® that was equipped with v) an injection port and viii) a level gauge confirmation window. The lower part had v) a load cell, vi) a level gauge, vii) an injection port and viii) a pore. The load cell was 1.0 mm high. The injection force was measured using an oscilloscope to convert pressure (1 N) to voltage (1 V). The distance was fixed at 8.0 mm from the nozzle tip of ShimaJet® to high-sensitivity load cells in TX-9UA.

Fig. 2

3.4 Release experiment from excised skin

The release test after topical injection of rhodamine 6G by ShimaJet® was performed using back skin excised from hairless rats. After the rats had been

anesthetized by intraperitoneal injection of sodium pentobarbital (50 mg/kg), the back skin was excised, as explained in our previous paper (Okumura et al., 1989). Rhodamine 6G solution (1.0 mg/mL, 100 μL) was injected into the excised skin by NIF-w or NFI-s at a constant load of 4.9 N. Next, the skin membrane was mounted in a Franz-type diffusion cell (effective diffusion area: 1.77 cm^2). The stratum corneum side was covered with Parafilm® and 6 mL of pH7.4 phosphate-buffered saline (PBS) was applied to the dermal side. Periodically, samples of 0.50 mL were taken from the dermal side compartment, and then the same volume of PBS was added to keep the volume constant. Rhodamine 6G concentration in the sample was determined by a fluorescence spectrophotometer (RF5300PC; Shimadzu) at excitation and emission wavelengths of 490 and 520 nm, respectively. All animal experiments were approved by the ethics committee at Josai University and carried out following the guidance of Josai University.

3.5. Observation of drug distribution in skin

Rhodamine 6G was injected into the excised skin by NFI-w or NFI-s. The treated skin was embedded in Tissue-TeK® O.T.C compound (Sakura Fine Tech, Osaka, Japan) and frozen, and horizontal or vertical sections of 20 μm thickness were prepared

using a cryostat (CM3050S; LEICA, Wetzlar, Germany). The distribution of rhodamine 6G in each specimen was observed with a fluorescence microscope (CK40; Olympus, Tokyo, Japan).

3.6. Measurement of rhodamine 6G concentration in skin

The back skin excised from hairless rats was minced with forceps immediately after topical injection of rhodamine 6G solution. The minced skin tissues were homogenized with a Polytoron homogenizer (Kinematica, Lucerne, Switzerland) in methanol, and centrifuged at 15,000 rpm for 3 min at 4°C. Rhodamine 6G concentration in the supernatant was measured using the fluorescence spectrophotometer. Furthermore, rhodamine 6G concentration in skin slices (20 μm thickness) was measured after extraction with methanol.

3.7 *In vivo* experiment

The time course of plasma concentration of rhodamine 6G was followed after intravenous bolus injection using a 27-gauge syringe or administration of the compound to hairless rat back skin with NFI-s at a dose of 1.0 mg/mL (100 μL). Blood samples were periodically withdrawn through the jugular vein. Blood samples were

centrifuged at 15,000 g for 5 min at 4°C to obtain plasma. Rhodamine 6G concentration in plasma diluted by saline was measured using a fluorescence spectrophotometer. Animal experiments were performed under anesthesia using *i.p.* injection of urethane.

3.8. Simulation

Plasma concentration-time profiles after injection of rhodamine 6G into rat back skin by NFI-s were simulated by following eq. 2.

$$V\frac{dC}{dt} = nkt^{n-1} - kel \cdot V \cdot C \tag{2}$$

where C is the plasma concentratiopn of rhodamine 6G and V and kel are the apparent volume of distribution and the elimination rate constant, respectively, of rhodamine 6G. The rate constant k was caluculated from eq. 1 and V and kel were obtained from the blood concentration-time profile after bolus intraveous administration.

3. RESULTS

3.1. Injection force –time profiles after injection by ShimaJet®

Figure 3a and b show the time course of injection force after injection using NFI-w and NFI-s, respectively, through a normal nozzle. Injection force increased with

an increase in the injection volume from 50 to 250 μL both in NFI-w and NFI-s treatment. The maximum injection force, however, was almost constant above 100 μL of the injection volume. The decreased profiles of injection force after achieving the maximum injection force were different between two injectors below and above 100 μL. Injection force immediately decreased after reaching the maximum pressure in the case of injection volume under 100 μL, whereas injection force gradually decreased and the duration of high injection force was dependent on the injection volume in the case of injection volume more than 100 μL. Figure 3c shows the time course of injection force after injection by NFI-s through a modified nozzle. The increase of injection force by the increase in injection volume with the modified nozzle showed the same tendency as using the normal nozzle. The maximum injection force after injection through the modified nozzle, however, was much lower than that through the normal nozzle.

Fig. 3

3.2. Amount of rhodamine 6G delivered into skin by ShimaJet®

Figure 4 summarizes the amount of rhodamine 6G delivered into the whole skin, epidermis and dermis. The amounts of rhodamine 6G delivered in the whole skin

by NFI-w and NFI-s through the normal nozzle were 50.1 and 72.8 μg, respectively. Rhodamine 6G was also detected in the nozzle and on the skin surface. Interestingly, the amount of rhodamine 6G delivered was much different between the two springs. NFI-w with a normal nozzle delivered rhodamine 6G to the shallow part of the skin, and the amount in the shallow skin was about 1.5 times higher than in the dermis, whereas NFI-s with a normal nozzle mainly delivered rhodamine 6G through the dermis. When NFI-s with a modified nozzle was used, only 9.5 μg rhodamine 6G was delivered into the whole skin and most of the compound was detected in the dermis.

Fig. 4

3.3. Observation of skin distribution of rhodamine 6G

Figure 5a and b show fluorescence micrographs with rhodamine 6G distribution in the skin after injections using NFI-w and NFI-s, respectively. Shallow distribution of rhodamine 6G was observed in the shallow part of the skin after injection using NFI-w. On the other hand, rhodamine 6G was observed in the whole skin area after injection using NFI-s. Rhodamine 6G distribution after injection uisng NFI-s with a modified nozzle was slightly observed in the skin and the fluorescence intensity

of rhodamine 6G was much weaker than that after injections using NFI-w and NFI-s with the normal nozzle (data not shown). Subsequently, only the normal nozzle was used in this experiment because the modified nozzle could not effectively deliver rhodamine 6G into the skin. Figure 5c and d show the amount of rhodamine 6G at different depths from the skin surface after injection uisng NFI-w and NFI-s with a normal nozzle. NFI-w mainly delivered rhodamine 6G into the shallow part of skin: Most of the rhodamine 6G was detected in the skin up to 500 μm deep from the skin surface. On the other hand, NFI-s homogeneously delivered rhodamine 6G into the skin; the amount of rhodamine 6G in the skin was consistently equal at different depths from the skin surface to the bottom of the dermis. These results of rhodamine 6G distribution at different depths corresponded to the results of fluorescence observation (Fig. 4).

Fig. 5

3.4. Evaluation of rhodamine 6G release from injected skin

Figure 6 and Table 1 show release profiles of rhodamine 6G from the skin depot produced by needle-free injection. The release rate constant, k, and the release

exponent, *n*, were calculated from the double logarithmic plot of the cumulative amount of rhodamine 6G released-time profiles. Table 1 summarizes the calculated *k* and *n* values. The *k* and *n* values for NIF-w were 1.18 h^{-1} and 0.7, respectively, whereas those of NFI-s were 10.5 h^{-1} and 0.5. The *k* value of NFI-w was much slower than that of NFI-s. Next, the effect of a skin-penetration enhancer, HPE-101, was investigated on the amount of rhodamine 6G released from its injected depot in the skin and on rhodamine 6G distribution. As a formulation, HPE-101 was added at a concentration of 1.0% to 1.0 mg/ml rhodamine 6G solution and homogenized to obtain an O/W typed emulsion. Figure 6 and Table 1 show the time course of the amount of rhodamine 6G released after injection of the O/W emulsion by NFI-s and rhodamine 6G release parameters from O/W emulsion-injected skin. The rhodamine 6G release decreased by injecting the O/W emulsion compared with the drug solution and the *k* and *n* values were 0.78 h^{-1} and 0.66, respectively. The amount of rhodamine 6G delivered into the skin was 36.9 μg, which was comparatively low regardless of NFI-s injection (data not shown).

Fig. 6, Table 1

3.5. Rhodamine 6G concentration in skin after release experiment

Figure 7 shows rhodamine 6G concentration in the skin 12 h after the release experiment using its solution or O/W emulsion. Figure 7a, b and c indicate the rhodamine concentration in the whole skin, epidermis and dermis, respectively. Interestingly, rhodamine 6G concentration fell markedly after injection using NFI-s compared to the results shown in Fig. 4b and c, whereas most rhodamine 6G remained 12 h after injection using NFI-w. Furthermore, rhodamine 6G was retained over 12 h for O/W emulsion-injected skin.

Fig. 7

3.6. Plasma concentration of rhodamine 6G after injection using NFI-s

The elimination kinetics of rhodamine 6G after bolus i.v. injection in rats obeyed the linear 1-compartment model (data not shown). The obtained elimination rate constant, *kel*, and distribution volume, *V*, were 1.15 h^{-1} and 2.0 L, respectively. Figure 8a shows the observed and simulated plasma concentrations after injection of 100 μL of 1.0 mg/mL rhodamine 6G solution by NIF-s to the back skin in rats. The simulated curve was obtained by eq. 2. The *C*max was observed 15 min after injection

and the plasma concentration gradually decreased over 5 h. The simulated curve did not correspond to the observed value, especially just after the injection. The simulated values were calculated under assumption that rhodamin 6G would be absorbed into cutaneous microvascular vessels just after it passed through the whole skin. These microvascular vessels, however, exist in the dermis, not at the end of the dermis. Thus in vivo absorption of rhodamin 6G must start a little earlier than in vitro reaching into the end of the dermis and part of rhodamin 6G might be directly absorbed just after its injection into the skin. Figure 8b shows the observed value and the sum of the simulated values calculated by eq. 2. The simulated values were assumed to be part of rhodamine 6G, which was directly transported from the skin into blood just after NFI-s injection. The amount of rhodamine 6G transferred into the blood was fixed at 11.8 μg. This summarized value was very close to the observed value. Thus, rhodamine was thought to be transported from the skin to the systemic circulation after NFI-s injection.

Fig. 8

4. Discussion

Breaking through the stratum corneum barrier is the key for developing TDDS. Traditional TDDS limited the molecular size of drugs to less than 500 Da, as explained by the 500 Dalton rule (Bos and Meinardi, 2000). Thus, the formulation of TDDS is not suitable for high molecule hydrophilic drugs, such as proteins and vaccines. Needle-free injection using ShimaJet® enabled not only direct drug delivery to the target site of the skin, but is also a systemic drug delivery system bypassing the stratum corneum barrier. Other physical approaches, such as microneedles (Prausnitz, 2004) and electroporation (Tokudome and Sugibayashi, 2004), have also been investigated as promising means to overcome the barrier function of the stratum corneum. Among these methods, needle-free injection would provide a high dose of drug into the skin. Many reports have been found on the effectiveness of a needle-free injector as a drug delivery device (Baxter and Mitragotri, 2005; Schramm and Mitragotri, 2002). Few studies, however, have reported the dermatokinetics and distribution of injected drugs after needle-free injection. On the other hand, several studies have reported the dermatokinetics of the drug and translocation to the systemic circulation from the injected site after subcutaneous injection (Yoshida et al., 2008 a,b). The drug disposition in the skin after subcutaneous injection was very different from after application of traditional TDDS. The amount of rhodamine 6G delivered to the

skin after injection of 100 μL of 1.0 mg/mL rhodamine 6G by ShimaJet® was greatly affected by the spring constant and nozzle type. The low value of the maximum injection force produced by NFI-w through a normal nozzle and NFI-s through a modified nozzle may not be enough to break through the stratum corneum barrier. The NFI-w injection, however, was capable of selectively delivering rhodamine 6G into the epidermis. Thus, the present results suggested that the ingenuity of device or formulation might be very important for selective drug delivery into the skin, but that improvement of the device will be required to increase the delivery amount of rhodamine 6G.

The release profiles of rhodamine 6G after injection using NFI-w and NFI-s were supposed to be diffusion-controlled and membrane-controlled, respectively (Ritger and Peppas, 1987). These different release profiles depended on the skin distributions after injection using NFI-w and NFI-s. The distributed rhodamine 6G might diffuse along different diffusion pathways into skin. Furthermore, the physicochemical characteristics of rhodamine 6G might also be related to the release profiles. A large volume of solution flowing into the skin at one time would alter the physicochemical and structural characteristics of the skin tissues. The pH of the skin surface and dermis is 4.5 to 5.5 and 7.2, respectively (Ohman and Vahlquist, 1998) and the pKa of rhodamine

6G is 7.5. Thus, rhodamine 6G mainly exists as a cation and might interact with negatively charged cutaneous cells in the epidermis. Application of a base such as lidocaine using NFI-w would show the early onset and long-acting effect (data not shown). Detail investigations are necessary to clarify the mechanism of drug release from the skin depot made by an NFI. The emulsion prepared using HPE-101 shows the unique characteristics of rhodamine 6G release from the depot. The amount of rhodamine 6G delivered to the skin after injection of the emulsion by NFI-s was lower than that after injection of rhodamine 6G solution. Although the amount of rhodamine 6G delivered was low after injection of the emulsion, the retention time of rhodamine 6G in the epidermis increased with a decrease in the release rate from skin. Emulsion delivery using an NFI might be effective for topically effective drugs, especially those having early onset and long-acting therapeutics. This method could be applicable also to biodegradable nano-/microsphere suspensions and liposome formulations.

Needle-free injection utilizes compressed gas to deliver drugs into skin (Mumper and Cui, 2003). We selected a device, ShimaJet ®, which utilizes a spring power system. The skin depth of the drug was controllable by modifying the nozzle shape. This modified nozzle could be used not only in the spring-powered device ShimaJet®but also in a compressed-gas-powered Biojector.

The injection volume and formulation administered into the cutaneous tissues had a great effect on the dermatokinetics of drugs (Yoshida et al., 2007). The NFI-s delivered a large amount of solution into the skin and this delivery technique might alter the dermatokinetics of the drug compared to traditional TDDS. The present results suggested that an NFI would be effective as a novel transdermal drug delivery system using the epidermis or epidermis/dermis as a drug depot or a drug release controlled reservoir. The theoretical blood concentration calculated using the in vitro release data was different from the observed values. This difference might be due to the migration of rhodamine 6G into microvascular vessels in the skin, suggesting that direct migration of the drug into the microvascular vessels was taking place after injection by NFI-s. Thus, NFI-w and NFI-s are useful devices for effective systemic and local delivery of drugs, respectively.

5. Conclusions

The depth of rhodamine 6G delivered into the skin and its release after injecton by ShimaJet® could be controlled by enhancing the spring constant, outlet shape of the nozzle and the formulation. In the present results, however, rhodamine 6G delivery through the modified nozzle and that using the emulsion indicated a lower drug

delivery rate compared to solution injection by NFI-s through the normal nozzle. Therefore, improvement of the delivery technique using ShimaJet® is required to obtain depth-controllable drug delivery. Currently, the relationships between the drug-delivery depth or the retention time of the drug in skin and the onset or lasting pharmacological effects are being investigated. In the future, efficient and controllable delivery will be obtained by needle-free injection.

Agerso H., Moller-Pedersen J., Cappi S., Thomann P., Jesussek B., Senderovitz T., 2002. Pharmacokinetics and pharmacodynamics of a new formulation of recombinant human growth hormone administered by ZomaJet 2 Vision, a new needle-free device, compared to subcutaneous administration using a conventional syringe. J. Clin. Pharmacol. 42, 1262-1268.

Bos J.D., Meinardi M.M., 2000. The 500 Dalton rule for the skin penetration of chemical compounds and drugs. Exp. Dermatol. 9, 165-169.

Baxter J., Mitragotri S., 2005. Jet-induced skin puncture and its impact on needle-free jet injections, experimental studies and a predictive model. J. Control. Release 106, 361-373.

Higuchi W.I., 1962. Analysis of data on the medicament release from ointments. J. Pharm. Sci. 51, 802-804.

Imoto J., Konishi E., 2005. Needle-free jet injection of a mixture of Japanese encephalitis DNA and protein vaccines: a strategy to effectively enhance immunogenicity of the DNA vaccine in a murine model. Viral. Immunol. 18, 205-212.

Inoue N., Kobayashi D., Kimura M., Toyama M., Sugawara I., Itpyama S., Ogihara M., Sugibayashi K., Morimoto Y., 1996. Fundamental investigation of a novel drug delivery system, a transdermal delivery system with jet injection. Int. J. Pharm. 137, 75-84.

Jackson L.A., Austin G., Chen R.T., Stout R., DeStefano F., Gorse G.J., Newman F.K.,

Yu O., Weniger B.G., 2001. Safety and immunogenicity of varying dosages of trivalent inactivated influenza vaccine administered by needle-free jet injectors. Vaccine 19, 4703-4709.

Jovanovic-Peterson L., Sparks S., Palmer J.P., Peterson C.M., 1993. Jet-injected insulin is associated with decreased antibody production and postprandial glucose variability when compared with needle-injected insulin in gestational diabetic women. Diabetes Care 16, 1479-1484.

Okumura M., Sugibayashi K., Ogawa K., Morimoto Y., 1989. Skin permeability of water-soluble drugs. Chem. Pharm. Bull. 37, 1404-1406.

Ohman H., Vahlquist A., 1998. The pH gradient over the stratum corneum differs in X-linked recessive and autosomal dominant ichthyosis, a clue to the molecular origin of the "acid skin mantle"? J. Invest. Dermatol. 111, 674-677.

Prausnitz M.R., 2004. Microneedles for transdermal drug delivery. Adv. Drug Deliv. Rev. 56, 581-587.

Schramm J., Mitragotri S., 2002. Transdermal drug delivery by jet injectors, energetics of jet formation and penetration. Pharm. Res. 19, 1673-1679.

Ritger P.L., Peppas N.A., 1987. A simple equation for desciption of solute release I. Fickian and non-Fickian release from non-swellable devices in the form of slabs, spheres, cylinders or discs. J. Control. Release 5, 23-36.

Theintz G.E., Sizonenko P.C., 1991. Risks of jet injection of insulin in children. Eur. J. Pediatr. 150, 554-556.

Tokudome Y., Sugibayashi K., 2004. Mechanism of the synergic effects of calcium chloride and electroporation on the in vitro enhanced skin permeation of drugs. J. Control. Release 95, 267-274.

Mumper R.J., Cui Z., 2003. Genetic immunization by jet injection of targeted pDNA-coated nanoparticles. Methods 31, 255-262.

Yoshida D., Todo H., Hasegawa T., Sugibayashi K., 2008a. Effect of molecular weight on the dermatopharmacokinetics and systemic disposition of drugs after intracutaneous injection. Eur. J. Pharm. Sci. 35, 5-11.

Yoshida D., Todo H., Hasegawa T., Sugibayashi K., 2008b. Effect of vasoactive agents on the dermatopharmacokinetics and systemic disposition of model compounds, salicylate and FITC-dextran 4 kDa, following intracutaneous injection of the compounds. Int. J. Pharm. 356, 181-186.

Yoshida D., Todo H., Hasegawa T., Sugibayashi K., 2007. Dermatopharmacokinetics of salicylate following topical injection in rats: effect of osmotic pressure and injection volume on salicylate disposition. Int. J. Pharm. 337, 142-147.

Table 1 Fickian release parameters of rhodamine 6G

	k (h^{-1})	n	Release type
NFI-w	1.18	0.70	Non-Fickan release
NFI-s	10.5	0.50	Fickian release
NFI-s (HPE-101)	0.78	0.66	Non-Fickan release

Figure Captions

Fig. 1 Diagram of normal and modified nozzles of ShimaJet ®.
a) Commercially available disposal nozzle: i) injection port, ii) nozzle-fixing bar, iii) screw thread, iv) solution-filling space.
b) Modified nozzle: v) injection port, vi) solution-filling space made of brass.

Fig. 2 Setup for TX-9A system to detect injection force of ShimaJet ®.
a) TX-9 system: i) digital oscilloscope, ii) sensor amplifier, iii) TX-9UA, iv) ShimaJet®. b) diagram of TX-9: v) load cell, vi) level gauge, vii) injection port, viii) pore.

Fig. 3 Effect of nozzle type and injection volume on the time course of injection force after injection by ShimaJet ®.
(a) NFI-w with normal nozzle, (b) NFI-s with normal nozzle, (c) NFI-s with modified nozzle
Lines: —: 50 μL, ····: 100 μL, —: 125 μL, ····: 250 μL for injection volume.

Fig. 4 Effect of nozzle type on the rhodamine 6G concentration in skin after injection by ShimaJet®.
Rhodamine 6G concentration in whole skin (a), epidermis (b) and dermis (c).
Gray column: NFI-w with normal nozzle, open column: NFI-s with normal nozzle, closed column: NFI-s with modified nozzle. Abbreviations: normal nozzle (NZ), modified nozzle (MN).

Fig. 5 Distribution of rhodamine 6G in skin after injection by NFI-w or NFI-s.
a) and b) fluorescence image of rhodamine 6G in the skin, c) and d) rhodamine concentration in the skin.

Fig. 6 Effect of formulations on rhodamine 6G release from rat skin after injection by NFI-s.
Symbols: ○: Injection of 1 mg/mL rhodamine 6G solution by NFI-s, ●: Injection of 1 mg/mL rhodamine 6G solution by NFI-w, □: Injection of 1mg/mL rhodamine 6G in 1% pirotiodecane by NFI-s

Fig. 7 Skin concentration of rhodamine 6G 12h after skin permeation experiment.

Rhodamin 6G concentration in whole skin (a), epidermis (b) and dermis (c).
Gray bar: Rhodamine 6G injection by NFI-w, white bar: rhodamine injection by NFI-s, black bar: rhodamine 6G with pirotiodecane injection by NFI-s.

Fig. 8 Plasma concentration of rhodamine 6G after NFI-s injection.
(a): observed (●) and simulated values obtained by eq. 2(○) .
(b): observed value (●), simulated value calculated by eq. (2) (○), simulated value after *i.v.* injection of rhodamine 6G (■) and the sum of that calculated by eq. (2) and the simulated value after *i.v.* injection of rhodamine 6G (△).

Figure 1

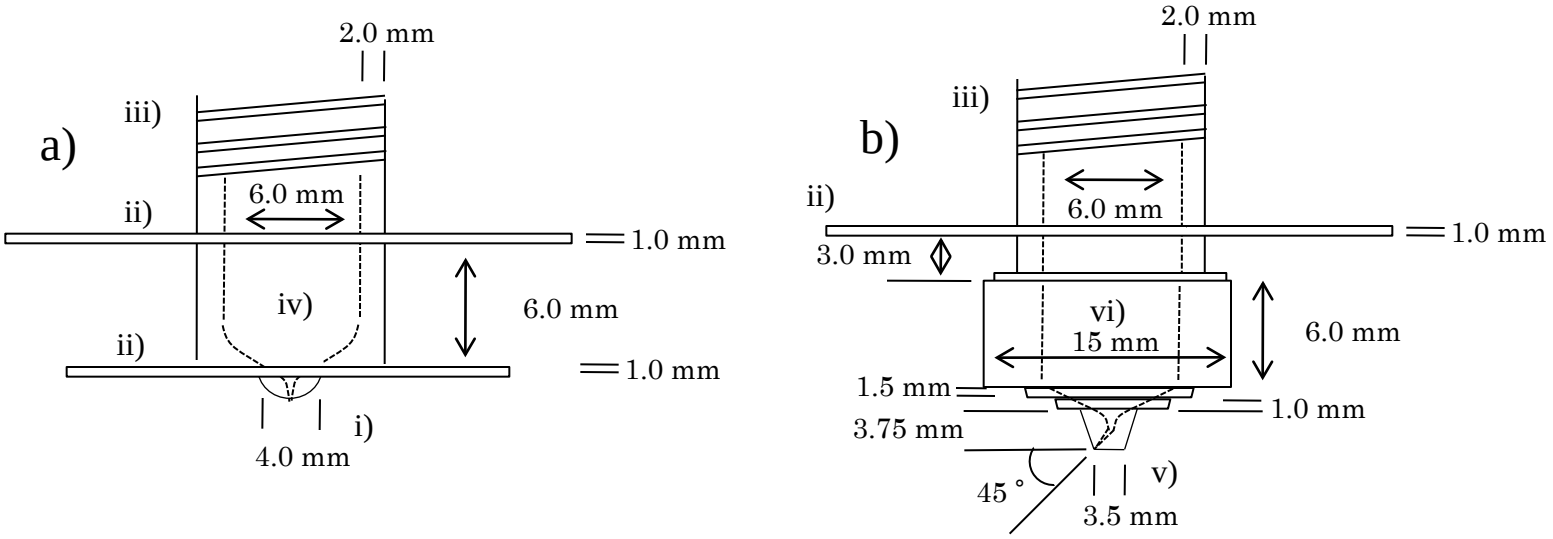
a)
2.0 mm
iii)
ii)
6.0 mm
1.0 mm
iv)
6.0 mm
ii)
1.0 mm
i)
4.0 mm
b)
2.0 mm
iii)
ii)
6.0 mm
1.0 mm
3.0 mm
vi)
15 mm
6.0 mm
1.5 mm
1.0 mm
3.75 mm
45 °
v)
3.5 mm

Figure 2

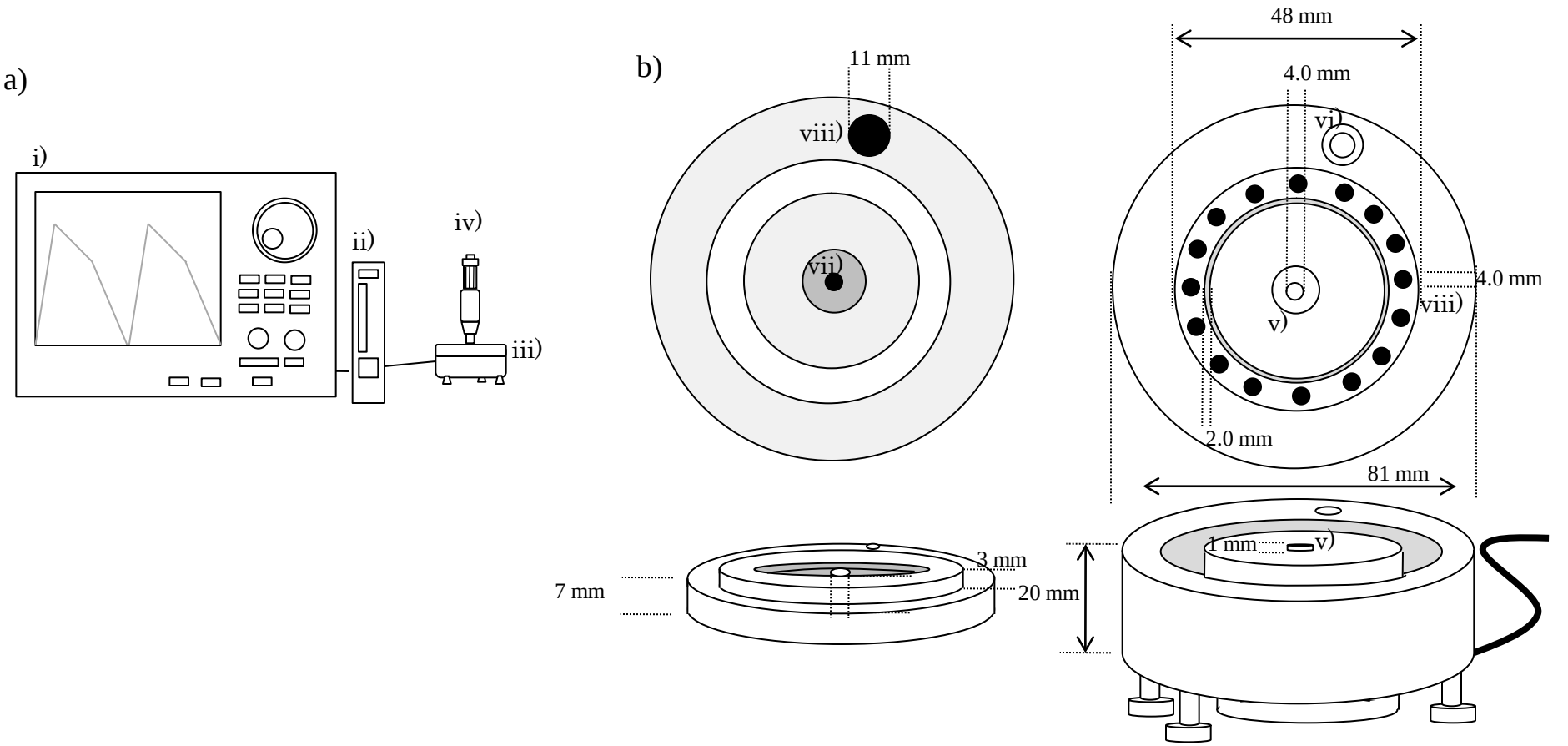
a)
i)
ii)
iii)
iv)
b)
11 mm
viii)
vii)
48 mm
4.0 mm
vi)
4.0 mm
viii)
v)
2.0 mm
81 mm
1 mm
v)
3 mm
7 mm
20 mm

Figure 3

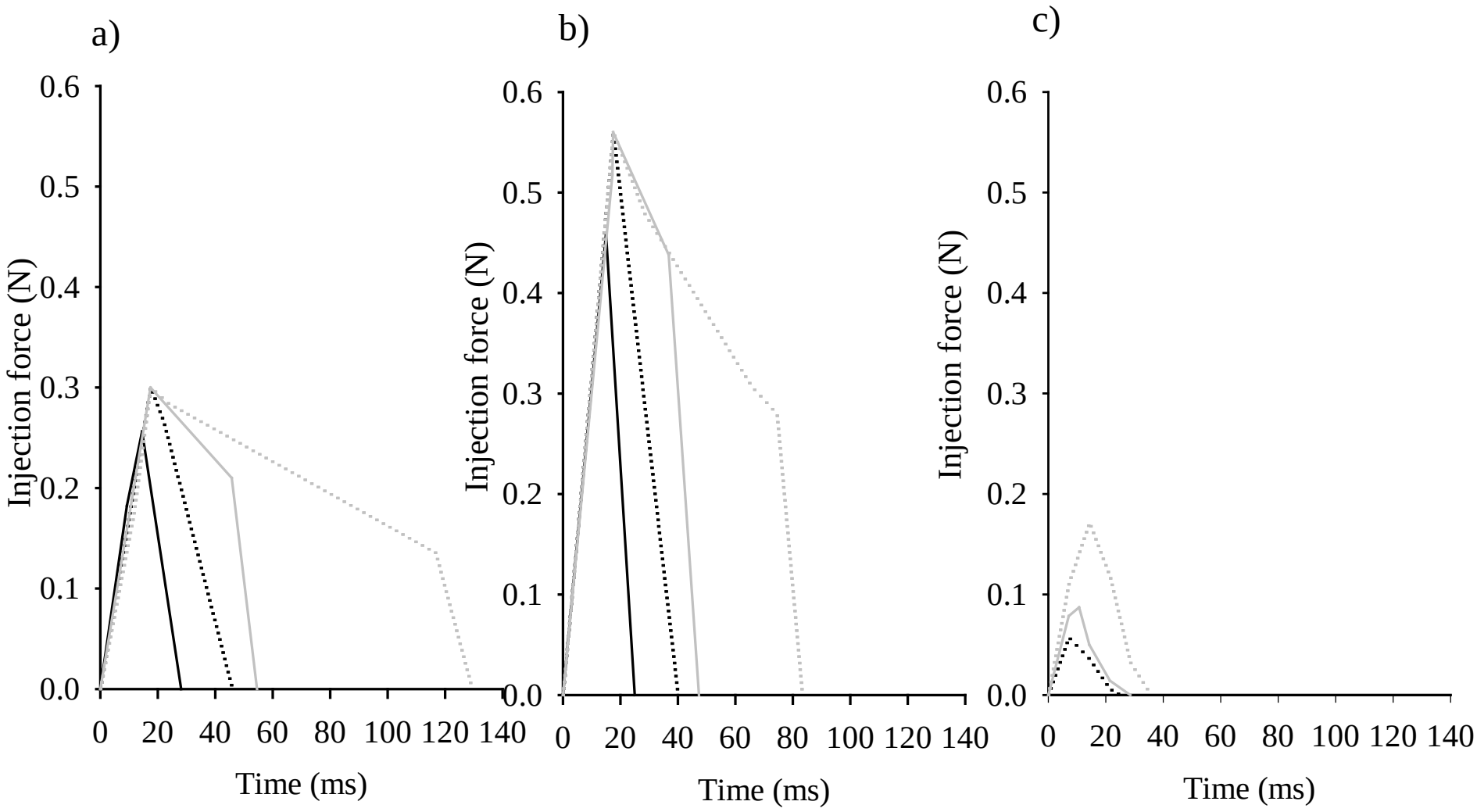
a)
b)
c)
Injection force (N)
0.0
0.1
0.2
0.3
0.4
0.5
0.6
0
20
40
60
80
100
120
140
Time (ms)

Figure 4

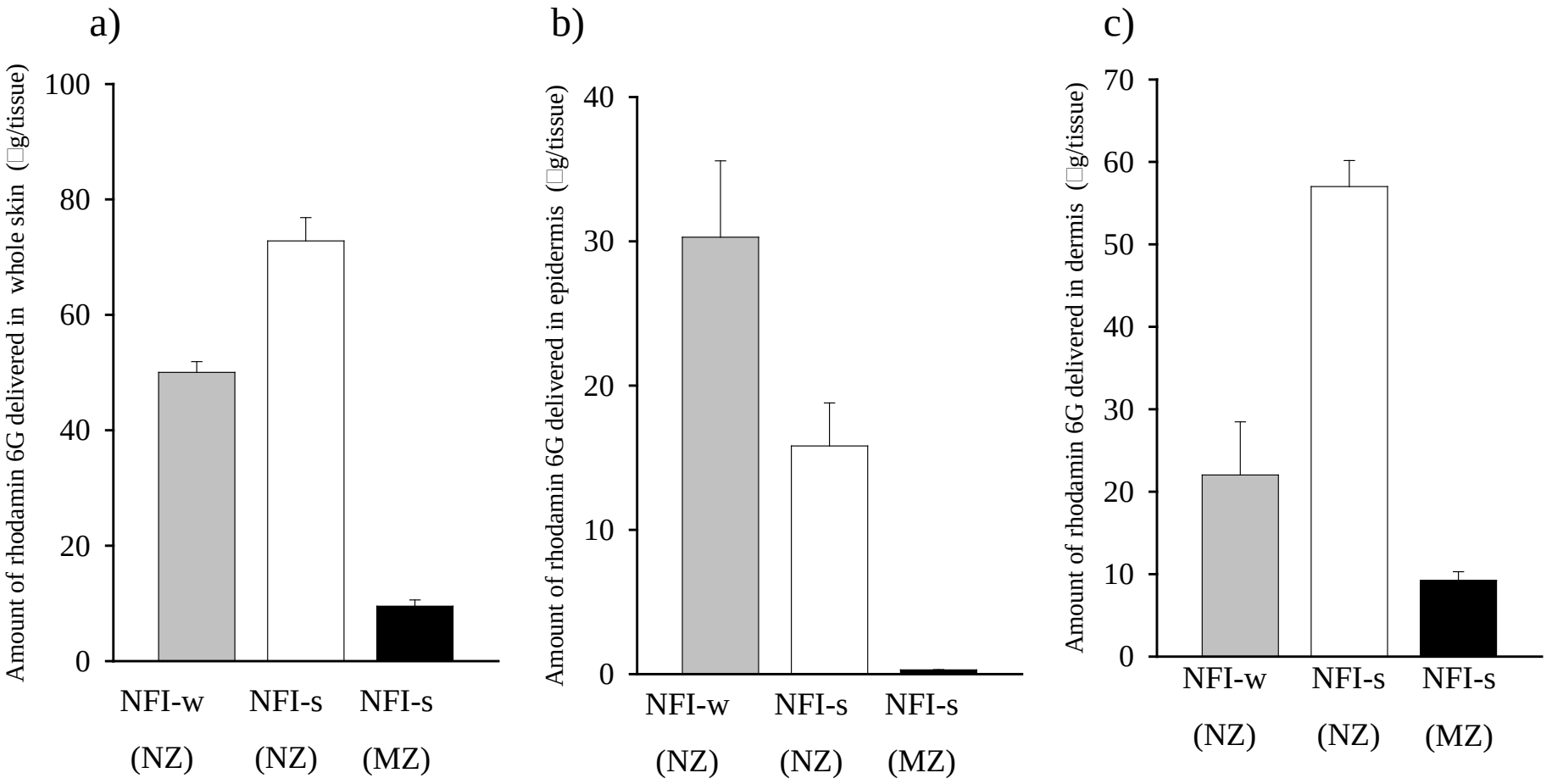
a)
Amount of rhodamin 6G delivered in whole skin (□g/tissue)
100
80
60
40
20
0
NFI-w (NZ)
NFI-s (NZ)
NFI-s (MZ)
b)
Amount of rhodamin 6G delivered in epidermis (□g/tissue)
40
30
20
10
0
NFI-w (NZ)
NFI-s (NZ)
NFI-s (MZ)
c)
Amount of rhodamin 6G delivered in dermis (□g/tissue)
70
60
50
40
30
20
10
0
NFI-w (NZ)
NFI-s (NZ)
NFI-s (MZ)

Figure 5

a) NFI-w

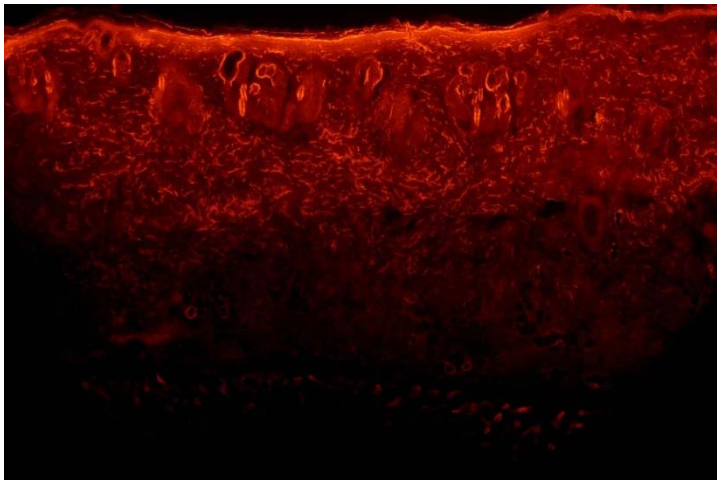

b) NFI-s

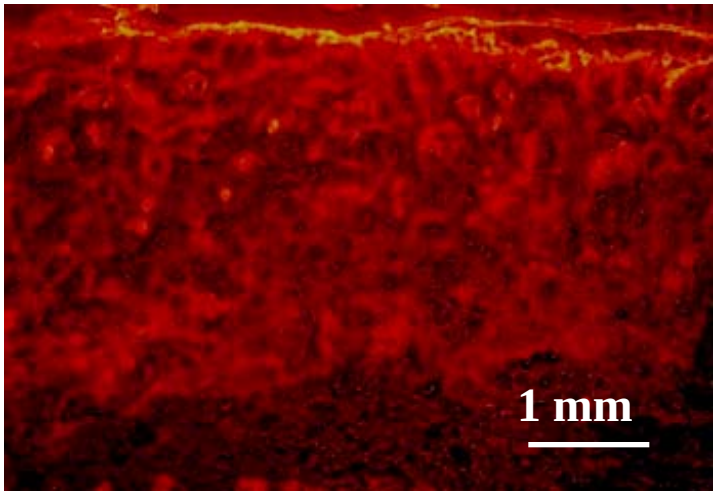

c)

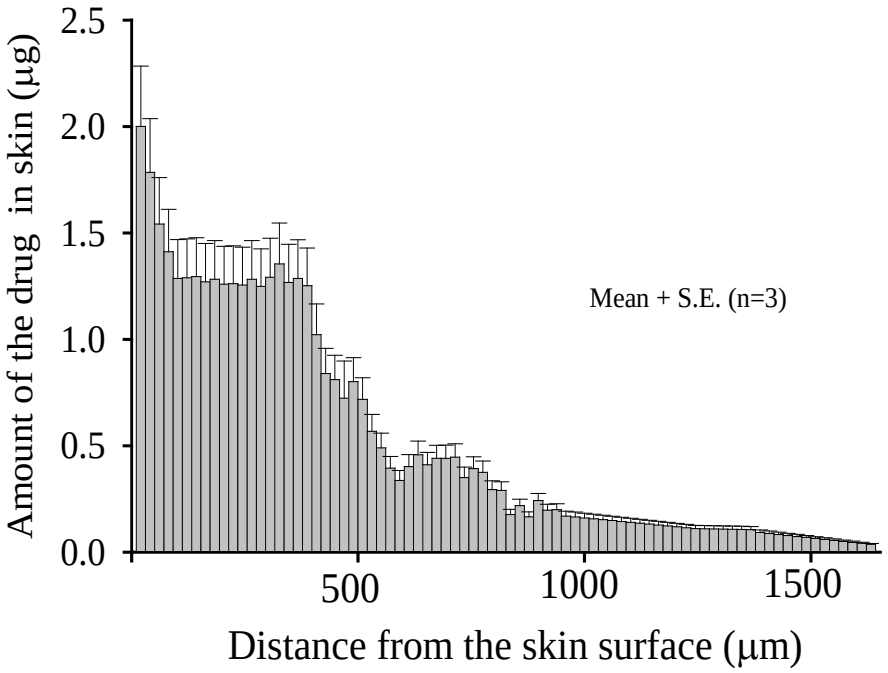

d)

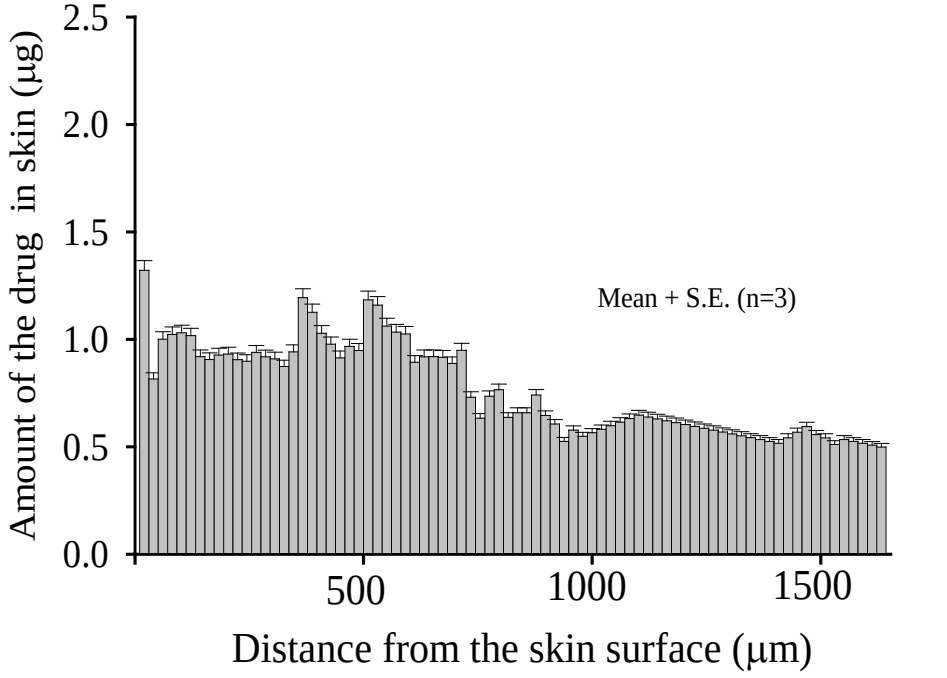

Figure 6

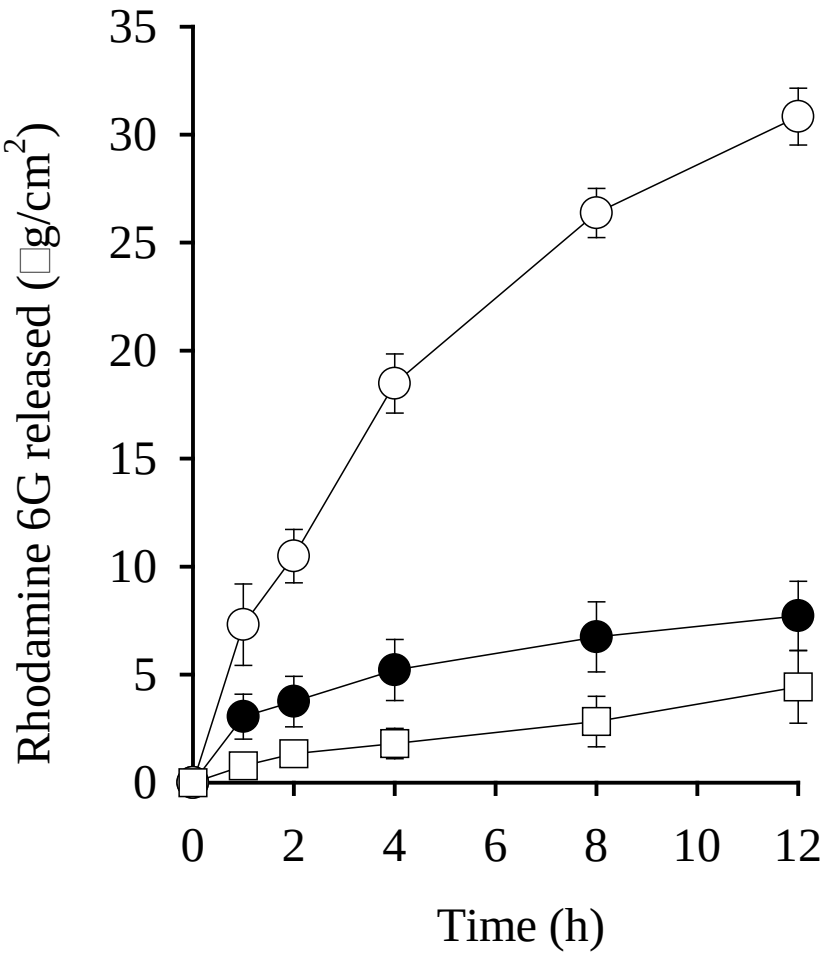
Rhodamine 6G released (□g/cm2)
35
30
25
20
15
10
5
0
0
2
4
6
8
10
12
Time (h)

Figure 7

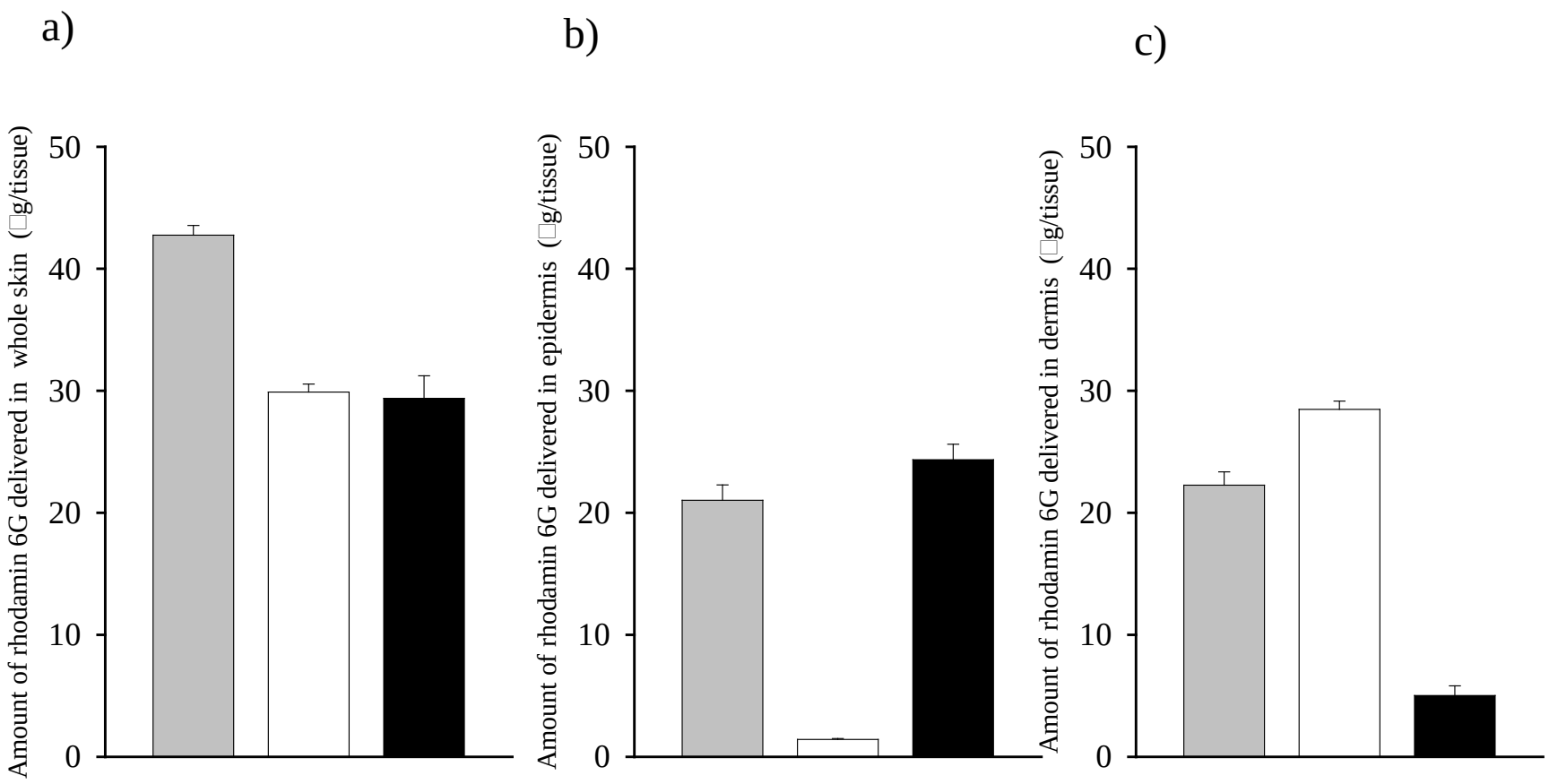
a)
b)
c)
Amount of rhodamin 6G delivered in whole skin (□g/tissue)
Amount of rhodamin 6G delivered in epidermis (□g/tissue)
Amount of rhodamin 6G delivered in dermis (□g/tissue)
0
10
20
30
40
50

Figure 8

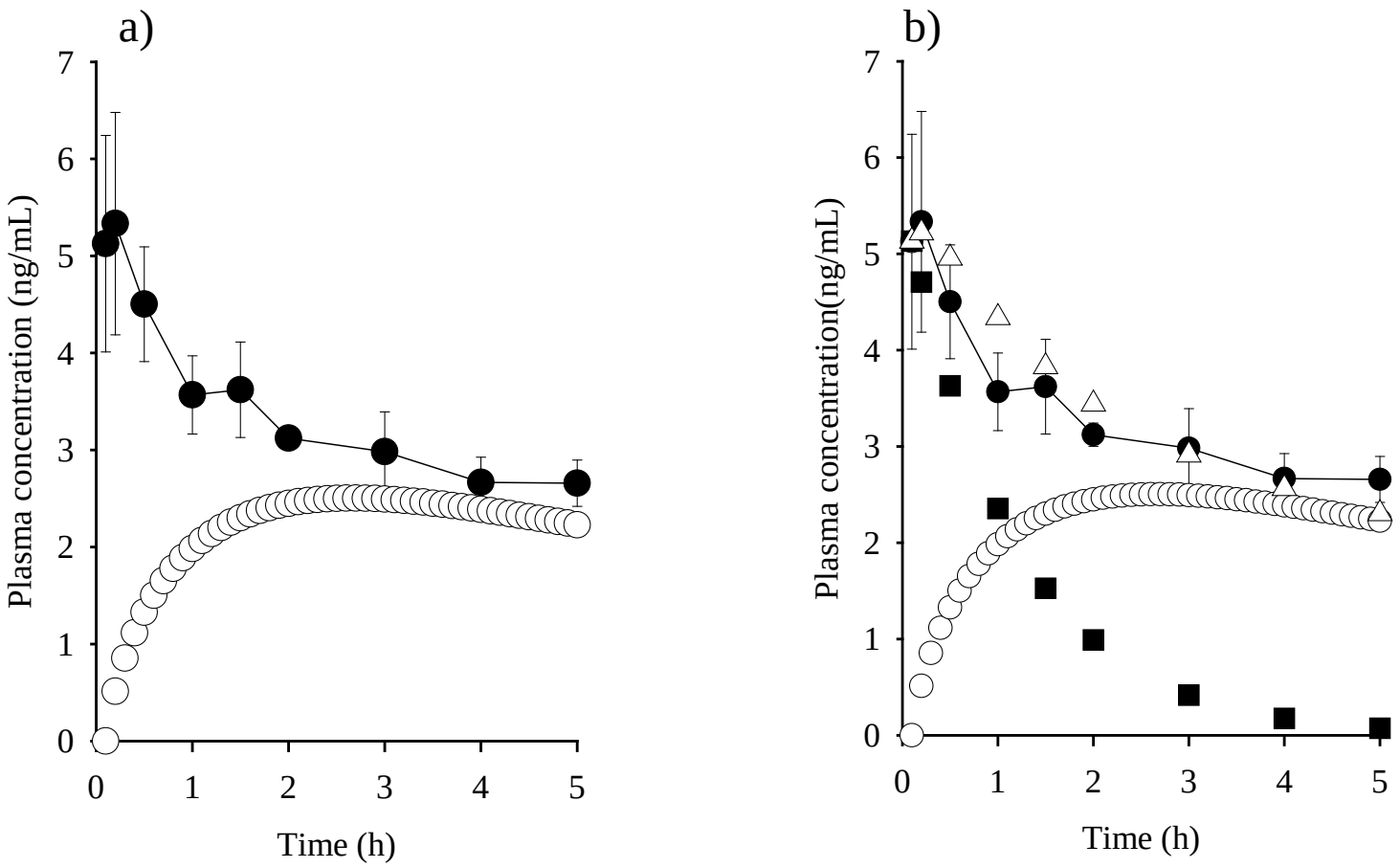
a)
b)
Plasma concentration (ng/mL)
Plasma concentration(ng/mL)
Time (h)
Time (h)
0
1
2
3
4
5
6
7